Two dimensional boundary value problem for the 2-nd order elliptic equation with discontinuous coefficient

V.A. Gordin, D.A. Shadrin

HSE & Hydrometeorological Center of Russia, Moscow,

vagordin@mail.ru, shadrin.dmitry2010@yandex.ru

Elliptic linear differential equations such as Poisson (1) and Helmholtz (2) equations describe stationary solutions (e.g. for diffusion, heat conductivity, and for distribution of the electrostatic potential)

$$L[u] = -div(\vartheta(\vec{x})grad(u)) = f(\vec{x}), \quad \vec{x} \in G, \tag{1}$$

$$L[u] = -div(\vartheta(\vec{x})grad(u)) + \rho(\vec{x})u = f(\vec{x}). \tag{2}$$

In many physical and technical cases, the media is not homogeneous and its properties (described by coefficients $\vartheta(\vec{x})$ and $\rho(\vec{x})$) are discontinuous.

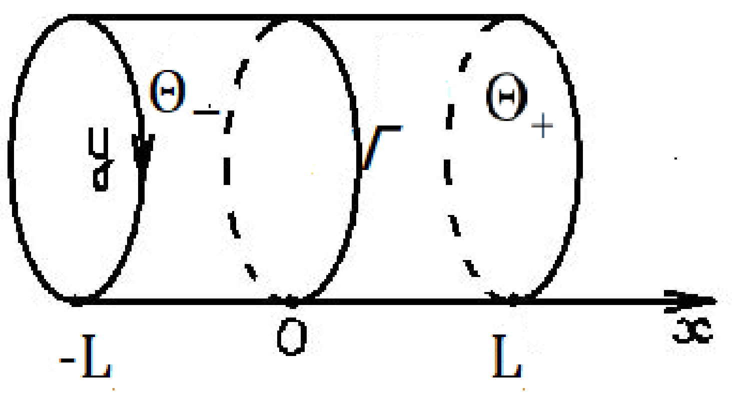

Fig. 1. Model: domain G – surface of the cylinder, jump-line Γ – central circle at $x = 0$, ϑ - piecewise continuous coefficient: ϑ_- in the left part of the cylinder, ϑ_+ - in the right. Here $x \in [-L, L],\ y \in [0, 2\pi)$.

On the edges of the cylinder G the Dirichlet boundary conditions are posed, on the jump-line Γ the Kirchhoff conditions are fulfilled:

$$[u] = 0, \qquad (3a) \qquad\qquad [\vartheta \partial_n u] = 0. \qquad (3b)$$

Here [ ] is an amplitude of the jump on line Γ, ∂_n is the normal derivative on Γ. We assume that $L = \pi$, in other cases we should renormalize our domain.

Grid in our experiments

The cylinder G is covered by a uniform grid with N knots on the circle and N+1 knots on its generatrix. Due to the chosen size the grid’s diameter in coordinates $<x, y>$ is equal to $h = \frac{2\pi}{N}$. Let us define for every point with the too dimensional index $\vec{j}$ of the grid a pair of difference operators $A_{\vec{j}}$ and $P_{\vec{j}}$, which approximate the differential problem (2 - 3) and are applied to the functions u and f, respectively, and a pair of stencils for these operators (grid points where operators have non-zero coefficients).

Compact approximation for equation *Lu*=*f* in a grid point $\vec{j}$

The operators $A_{\vec{j}}$ and $P_{\vec{j}}$ should be exact on a set of test functions: (u_k, f_k), where k=1,…,K, $f_k = L[u_k]$, L is the differential operator in the left-hand side of Eq. (1). Therefore $\forall k\ A_{\vec{j}} u_k = P_{\vec{j}} f_k$. Coefficients of the operators $A_{\vec{j}}$ and $P_{\vec{j}}$ for any grid index i are found by solving a “local SLAE” of order K+1. These coefficients form $|\vec{j}|$-th lines of the “global SLAE” $\mathbf{A}\vec{U} = \mathbf{P}\vec{F}$, where $\vec{U}$ is a finite-difference solution on the grid, $N \times (N+1) \gg K$. At points at the edge of G boundary conditions are approximated. $A_{\vec{j}}$ and $P_{\vec{j}}$ have non-zero coefficients only at K points of their stencils, all the other elements of line $|\vec{j}|$ in the global SLAE are zeros. As $K \ll N$, matrixes of the global SLAE are rather sparse.

The grid points are divided into four groups due to approximation method

Type I – points inside *G* far from *Γ*   *Точки внутри области далеко от Γ*

Type II – points, which stencils intersect with *Γ*   *Точки внутри области рядом с Γ*

Type III – points on line *Γ*   *Точки на Γ*

Type IV – points on the edges of *G*   *Точки на краях цилиндра* G - *далеко от Γ*

Points of type I

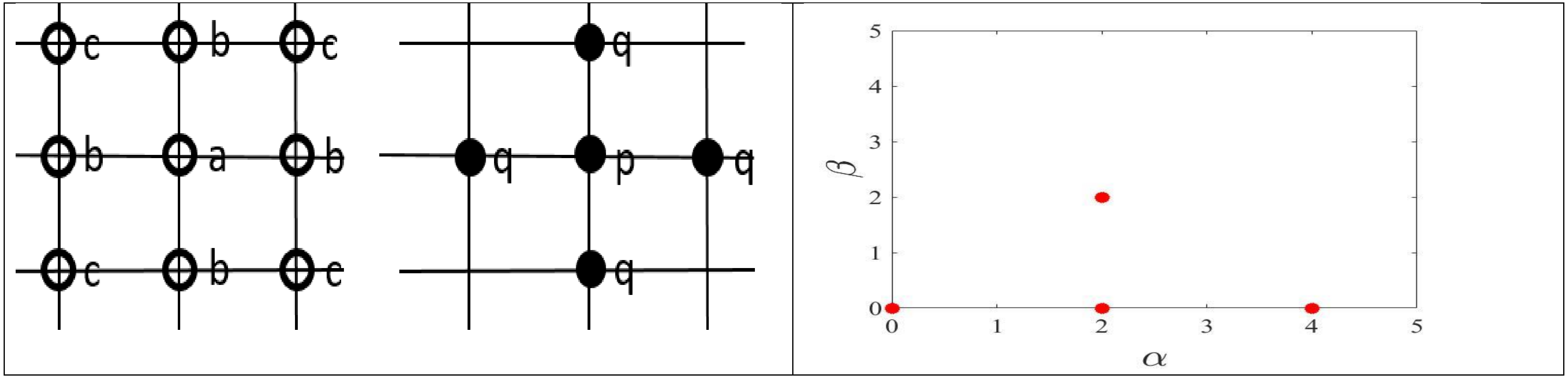

Fig. 2. *In the left part the scheme's stencils are presented and a Newton's diagram in the right part for monomials* $u_{\alpha\beta} = x^{\alpha} y^{\beta}$.

Let us use monomial $x^{\alpha} y^{\beta}$ as test functions. Due to the symmetry of the stencils with respect to vertical and horizontal axis, the monomials powers α, β are even. As the grid's diameters with respect to x and y are equal, the equations for test functions $x^{\alpha} y^{\beta}$ and $x^{\beta} y^{\alpha}$ will also be the same. That is why to achieve 4-th accuracy order we need to take only the following test functions: $1,\ x^2,\ x^4,\ x^2 y^2$.

The coefficients will be as follows: $a = 1,\ b = -0.2,\ c = -0.05,\ p = 0.2h^2,\ q = 0.025h^2$.

Points of type II

For points near to line Γ one should take the same stencils as for point of type I (view Fig.2). At the same time one should take in account that the right-hand side f is not defined on Γ, but there exist left and right-hand limits: f_- and f_+, respectively. Therefore, when constructing the global SLAE, we assume for point to the left from Γ the right-hand side is equal to f_-, and for points to the right from Γ the right-hand side is equal to f_+

Points of type III

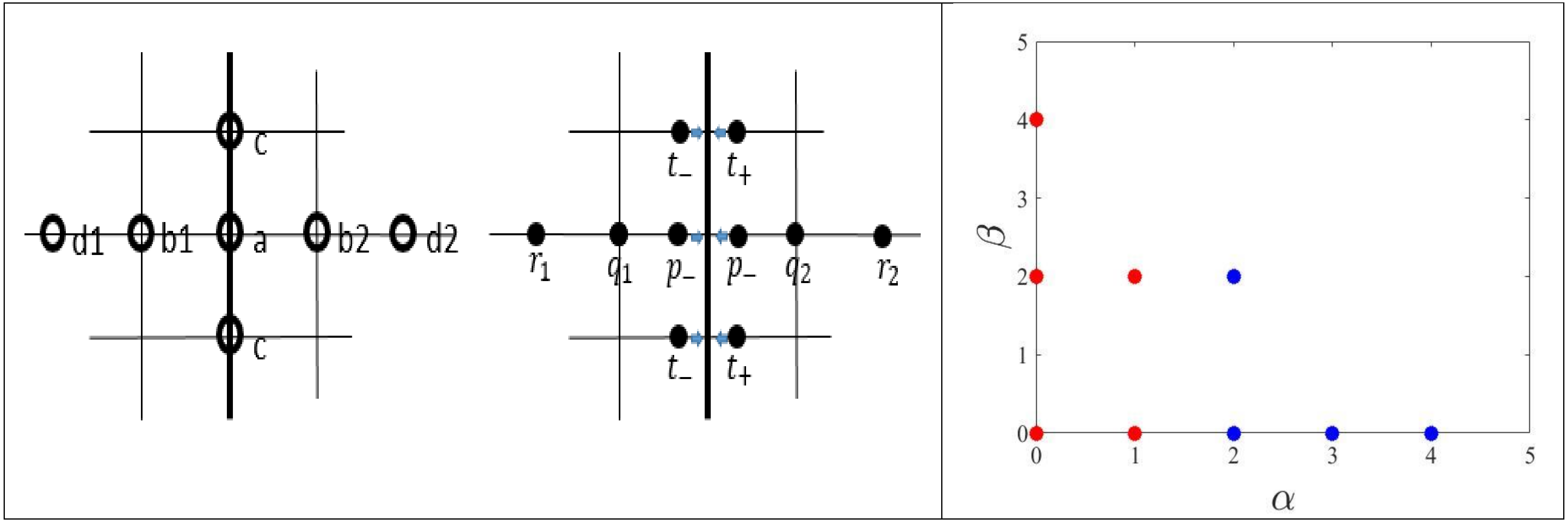

Fig.3. *Stencils and a Newton's diagram for points of type III. Blue points correspond to pair of test functions: one monomial with multiplier* ***sign****(x) and one monomial without it.*

We assume that the solution of the differential problem u is a piecewise analytic function, which has two different Taylor series on the right and on the left side from line Γ:

$$u(x,y)=\sum a_{ij}x^i y^j,\ x\le 0$$

$$u(x,y)=\sum b_{ij}x^i y^j,\ x\ge 0$$

From Kirchhoff conditions (3a,b) we obtain: $a_{0j} = b_{0j}$, $\vartheta_- a_{0j} = \vartheta_+ b_{0j}$. We chose the following test functions: $1, \dfrac{x}{\vartheta}, x^2, sign(x)x^2, x^3, sign(x)x^3, x^4, sign(x)x^4, y^2, \dfrac{y^2 x}{\vartheta}, x^2 y^2, sign(x)x^2 y^2, y^4$.

Here we also use the symmetry of the stencils with respect to horizontal axis.

The right-hand side on line Γ is a two valued function (f_+ and f_-), that is why the stencil for f has two coefficients on the jump-line Γ t_- & t_+, p_- & p_+). Coefficients t_-, p_- refere to the left-hand limit (f_-) and t_+, p_+ to the right-hand limit (f_+) .

After solving the “small SLAE” we obtain the following coefficients for the compact approximation:

$$a = 1,\ c = -\frac{1}{5},\ b_1 = -\frac{2\vartheta_+}{\vartheta_+ + \vartheta_-},\ b_2 = -\frac{2\vartheta_+}{\vartheta_+ + \vartheta_-},\ d_1 = \frac{\vartheta_-}{15(\vartheta_+ + \vartheta_-)},\ d_2 = \frac{\vartheta_+}{15(\vartheta_+ + \vartheta_-)},$$

$$r_1 = r_2 = -\frac{h^2}{36(\vartheta_+ + \vartheta_-)},\ \ q_1 = q_2 = -\frac{7h^2}{90(\vartheta_+ + \vartheta_-)},\ \ t_- = t_+ = \frac{h^2}{60(\vartheta_+ + \vartheta_-)},\ \ p_- = p_+ = \frac{7h^2}{60(\vartheta_+ + \vartheta_-)}.$$

Here at grid points of type IV – Dirichlet boundary condition

Constructions of the “global SLAE”

After calculating the coefficients of difference operators at each point the “global” matrices ***A*** and ***P*** are constructed. ***A*** is a square matrix, its size is $M \times M$ (M – number of grid’s knots). Matrix ***P*** counts points on Γ two times, as (f) is a two-valued function, therefore the size of ***P*** is $M \times (M + N)$.

To solve the SLAE we invert the matrix ***A***, that is why it is important to provide a good conditionality of ***A***. Local operators A_i are exact on the constant test function, therefore $\forall i \ \sum_j a_{ij} = 0$. If $a_{ii} > 0$, and all other weight are negative, then:

$$\sum_{j \neq i} |a_{ij}| = a_{ii} \ . \qquad (4)$$

Then zero lies on the boundary of Gershgorin’s circles, which contain the spectrum of ***A***. At boundary points of cylinder G the diagonal of ***A*** dominates. Therefore, one can hope that 0 won’t be included in ***A***’s spectrum, and the matrix ***A*** is invertible.

Tests, confirming the scheme's 4-th order.

The scheme's order can be evaluated the following way. We consider a smooth function $\tilde{u}$ and construct a new function $u(x,y) = g(x,y)\tilde{u}(x,y)$, where g – is a piecewise linear function by x: $g(x,y) = 1 + a(y)(x + |x|)$. Function $a(y)$ is defined so that u fulfills the Kirchhoff conditions (3a, 3b). Therefore $a(y) = \partial_x \tilde{u}(0,y) \dfrac{\vartheta_- - \vartheta_+}{2\vartheta_+ \tilde{u}(0,y)}$. Then we calculate f as $f = L[u]$, so u is the exact solution of problem (2-3) with the right hand-side f and suitable non-homogeneous Dirichlet boundary conditions.

The norm of the error (E) is evaluated as follows: $E = \left\| u_{appr} - u \right\|_C$. Here u_{appr} is a solution that is calculated by the difference scheme for the same right-hand side *f*. Below the graphs of errors depending on *N* are presented for three schemes: classic, compact, and compact with Richardson extrapolation. Experiments proving the scheme's accuracy order were made for huge coefficient: $\kappa = 10000$.

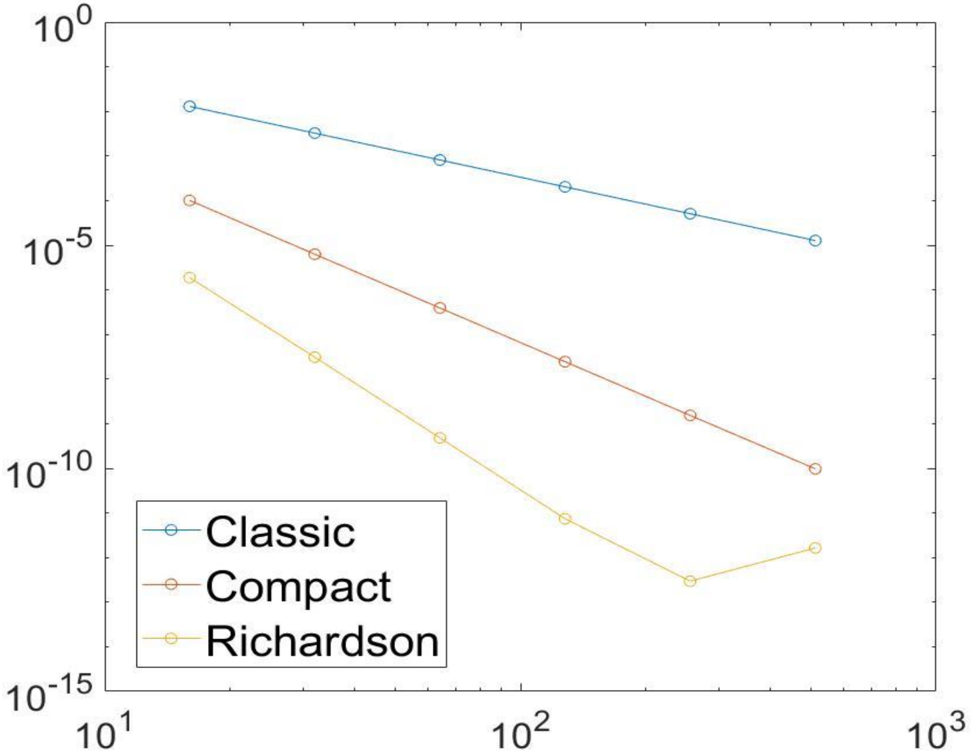

Fig.4. *The schemes' error depending on the number N in loglog coordinates. The exact solution:*

ũ – линейная функция;

$$u = \begin{cases} \vartheta_+ x \sin(y), & x \le 0 \\ \vartheta_- x \sin(y), & x \ge 0 \end{cases}.$$

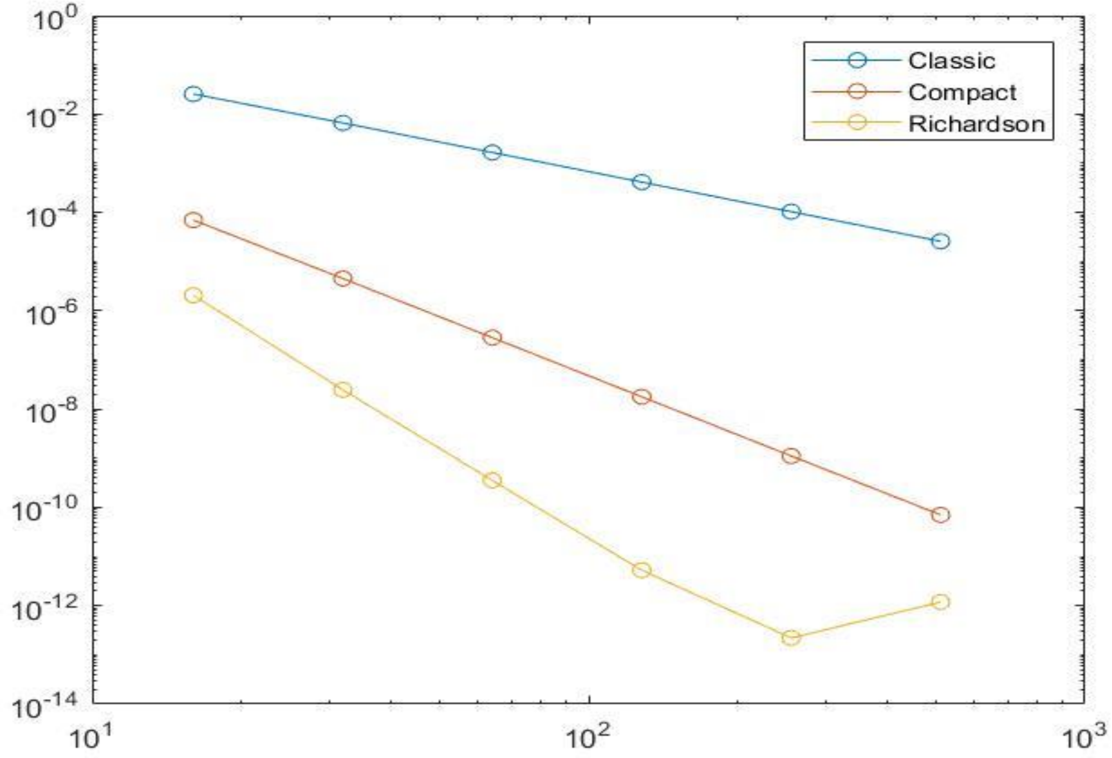

Fig.5. *The same results for the exact solution:*

$$\tilde{u} = x^6 \sin(y).$$

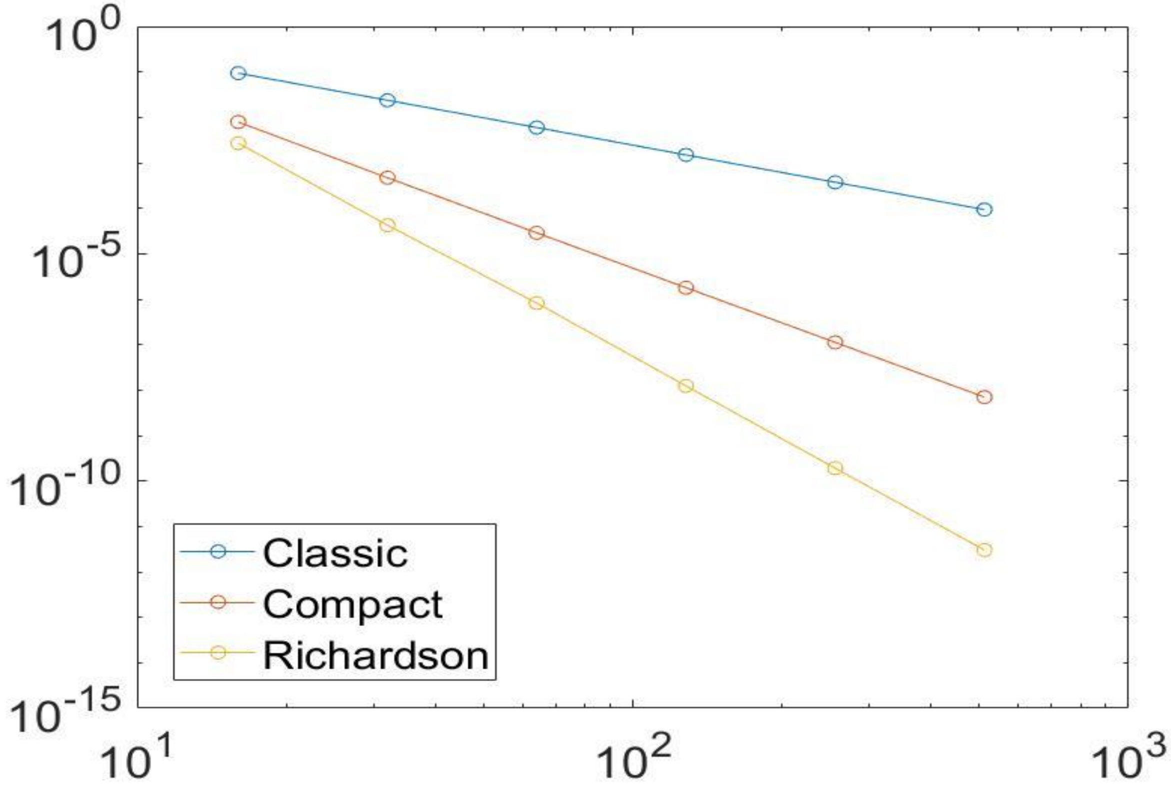

Fig.6. *The same results for the exact solution:*

$$\tilde{u} = \sin(y + x) + 2\,.$$

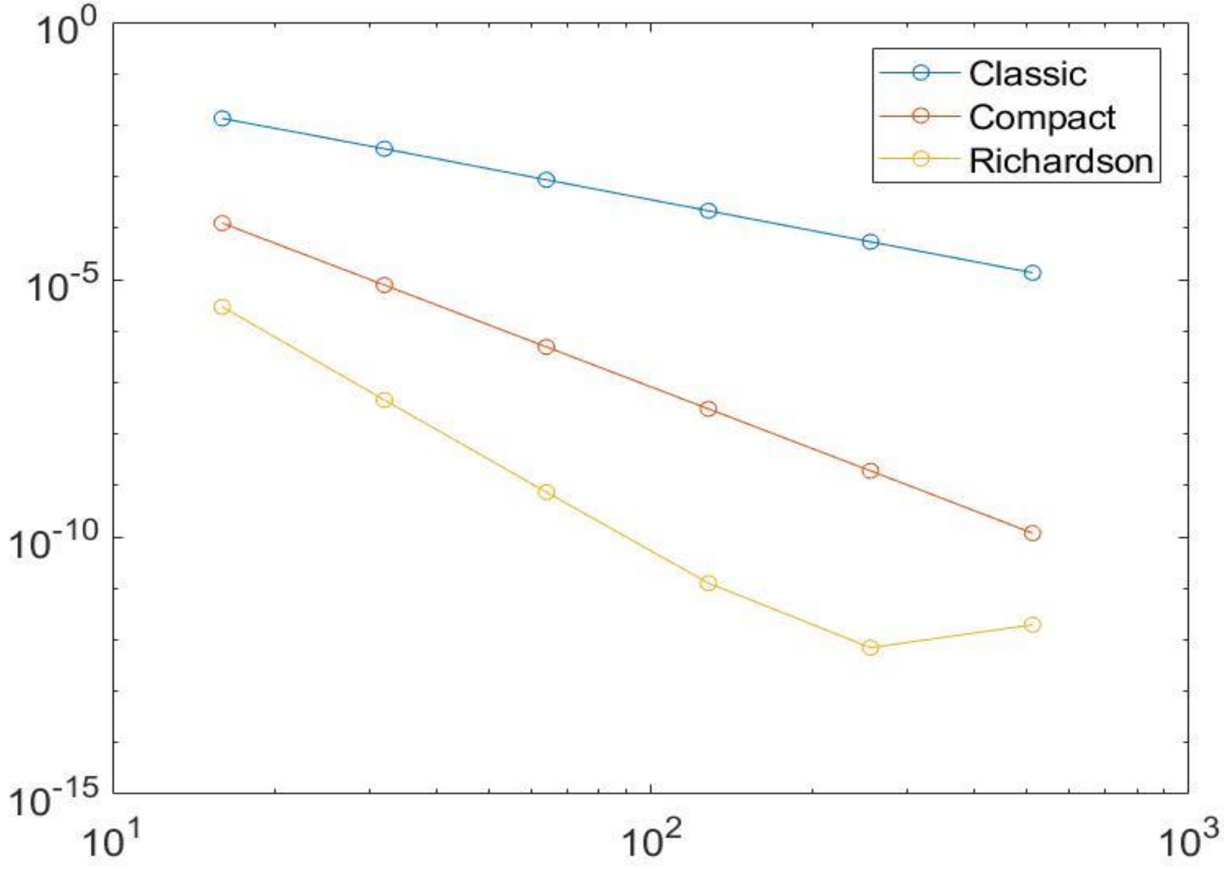

Fig.7. *The same results for the exact solution:*

$\tilde{u} = \sin(x)$

A sample solution of the Dirichlet problem.

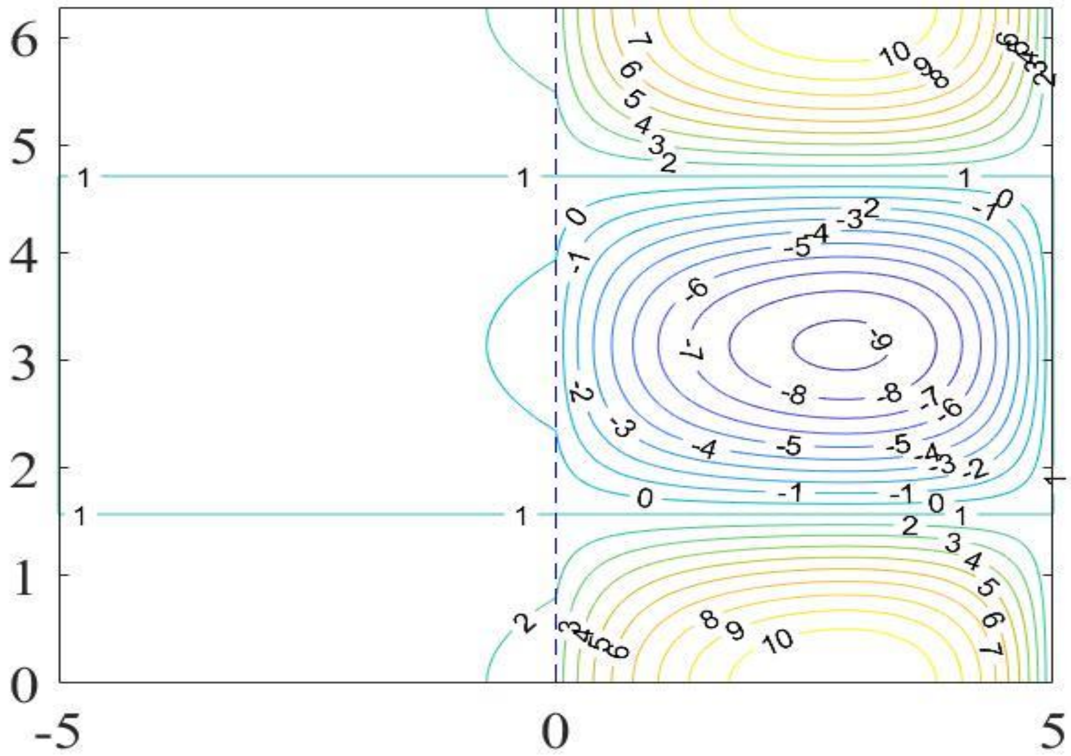

Fig.8. *Isolines of a sample solution at* $\kappa = 10$ *, right-hand side* $f = \cos(y)$ *and boundary conditions* $U(L, y) = U(-L, y) \equiv 1$ *This picture was drawn for N = 100.*

Experiments for homogeneous media

In this case the jump-line is absent and all grid point have either type I or IV. The stencils for inner points of G are shown on Fig.2.

For an exact solution *u* one can take any function from C^4. Below the results of numerical experiments are presented.

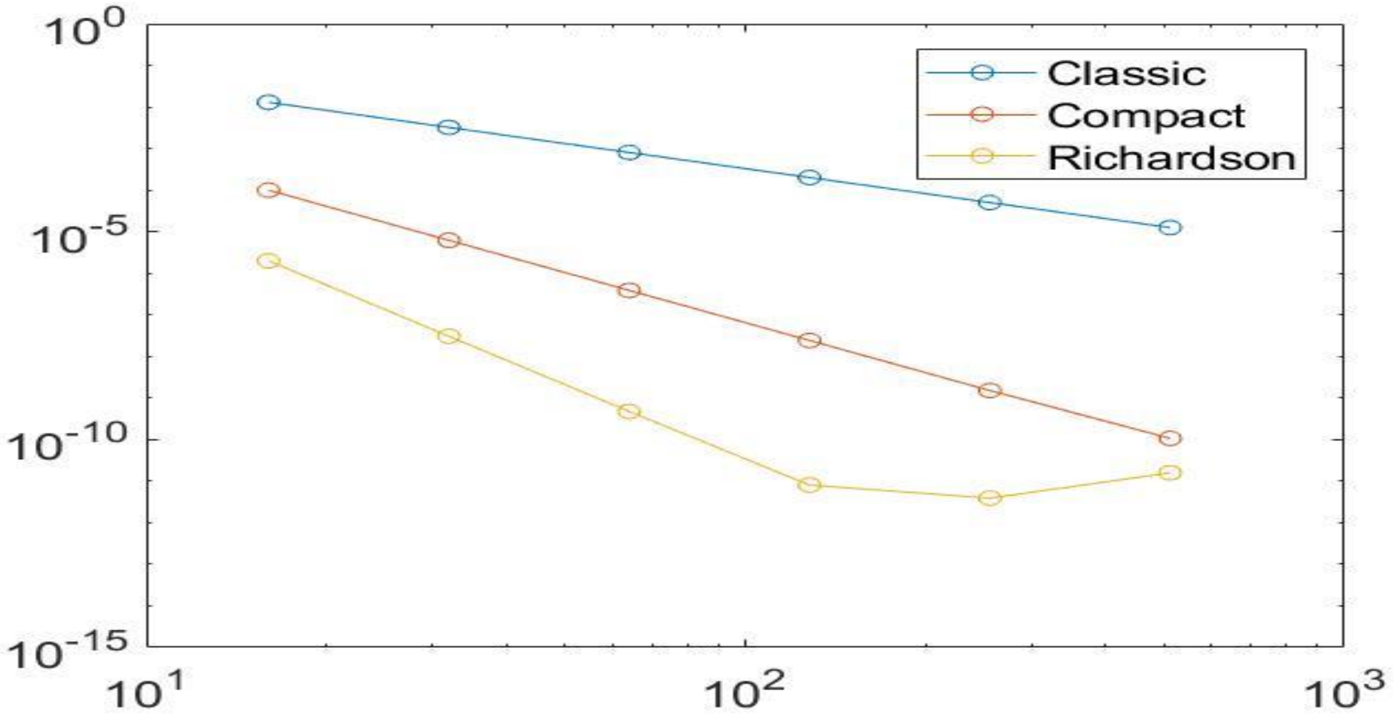

Fig.9. *The schemes' error depending on N in loglog coordinates. The exact solution:* $\tilde{u} = \sin(x)$

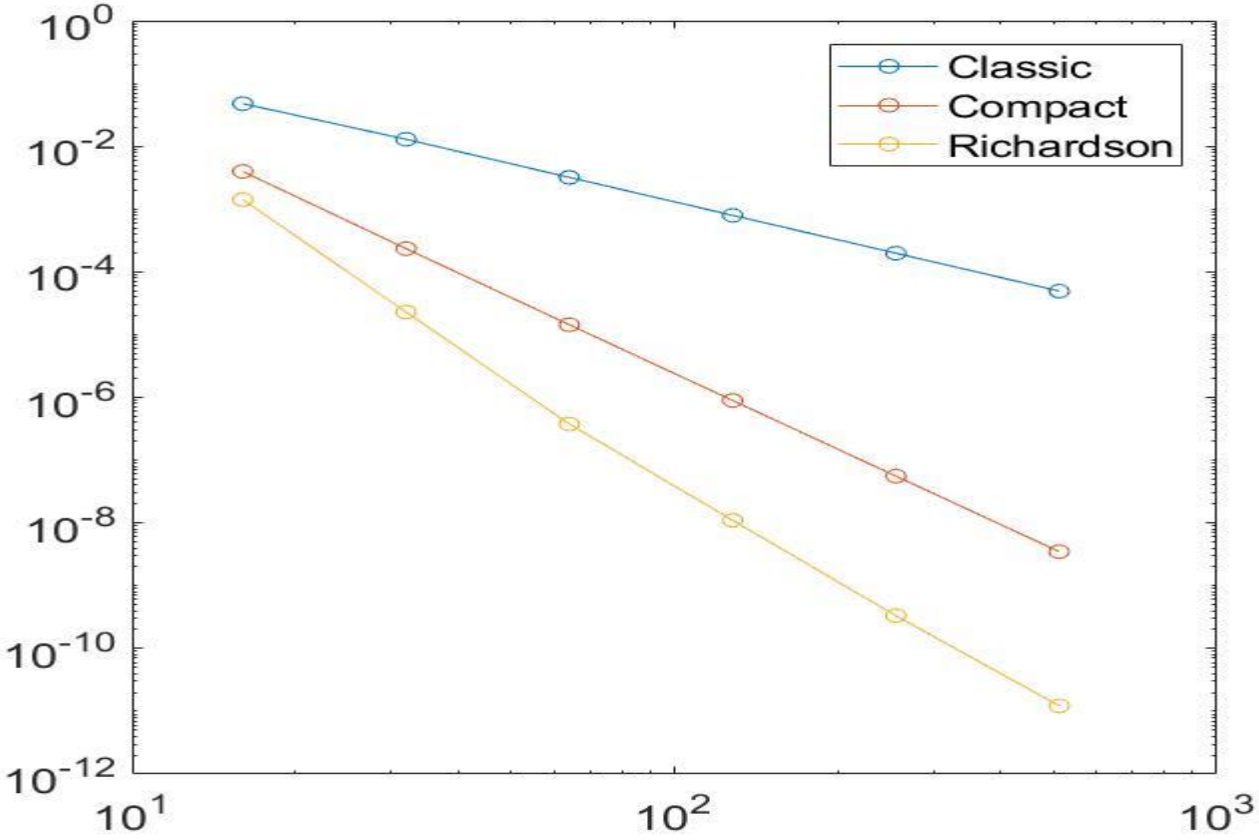

Fig.10. *The same results for the exact solution:* $\tilde{u} = \sin(x + y)$

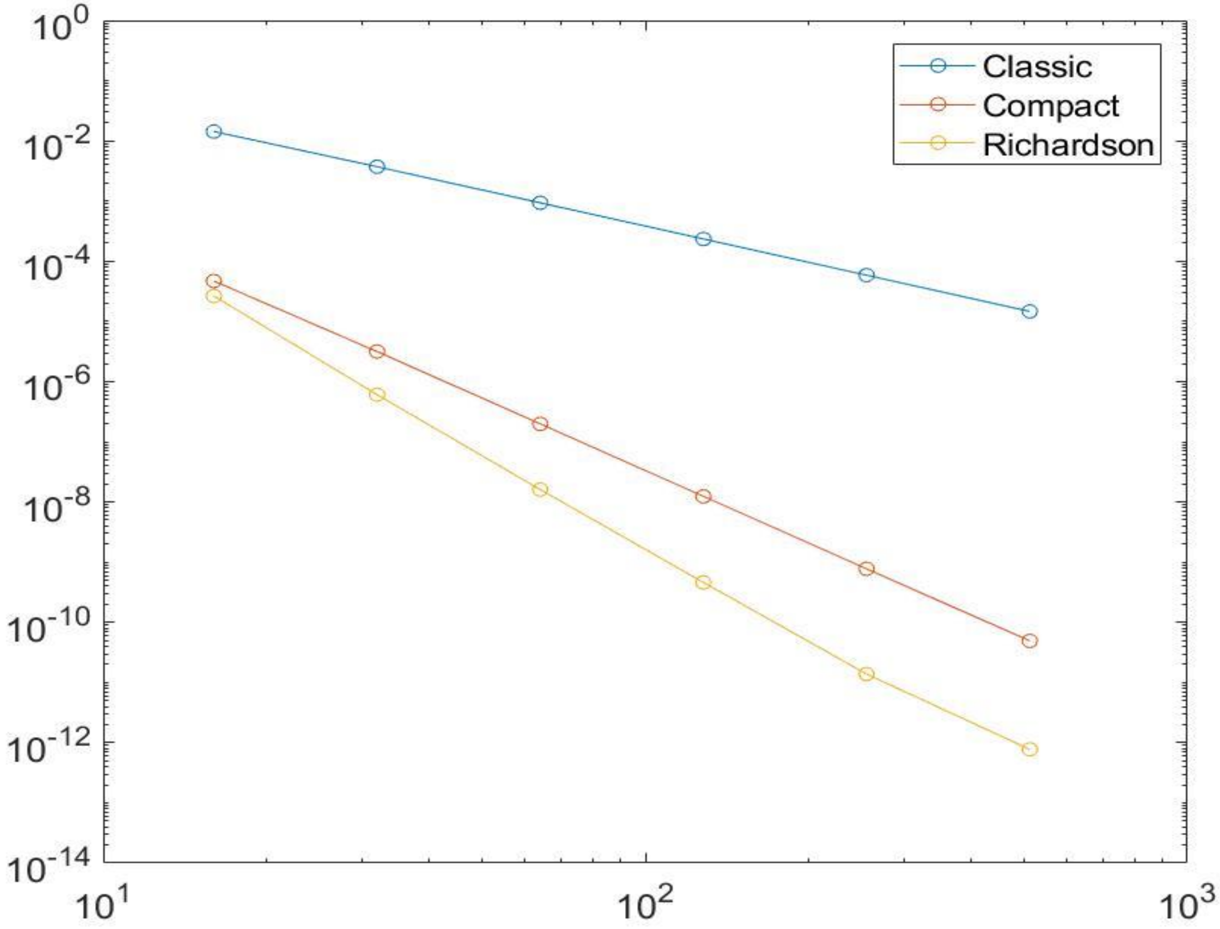

Fig.11. *The same results for the exact solution:* $\tilde{u} = x^6 \sin(x)$

Classic divergent scheme (in comparison with the compact one)

The idea of this scheme is in difference approximation of the derivatives as follows:

$$(u_x{}')_{i-1/2,j} \approx \frac{u_{ij} - u_{i-1,j}}{h}, \qquad (u_y{}')_{i,j-1/2} \approx \frac{u_{ij} - u_{i,j-1}}{h}.$$

Therefore, we get the following approximation of the Laplace operator:

$$(\bar{L}[u])_{ij} \approx h^{-2}\left\{\left[\vartheta\left(i+\frac{1}{2},j\right)\left(u_{(i+1),j}-u_{i,j}\right)-\vartheta\left(i-\frac{1}{2},j\right)\left(u_{i,j}-u_{(i-1),j}\right)\right]+\right.$$
$$\left.+\left[\vartheta\left(i,j+\frac{1}{2}\right)\left(u_{i,(j+1)}-u_{i,j}\right)-\vartheta\left(i,j-\frac{1}{2}\right)\left(u_{i,j}-u_{i,(j-1)}\right)\right]\right\}$$

At points of type **I** and **II** equation (1) is approximated: $\vartheta L[u]_{ij} = f_{ij}$.

At points of type III one can approximate the solution with two quadratic polynomial from each side of Γ and write the Kirchhoff condition (3), which will give the following relation between the polynomials’ coefficients:

$$\vartheta_- u_{i-2\,j} - 4\vartheta_- u_{i-1\,j} + 3(\vartheta_- + \vartheta_+)u_{ij} - 4\vartheta_+ u_{i+1\,j} + \vartheta_+ u_{i+2\,j} = 0. \qquad (5)$$

Richardson extrapolation

Our algorithm that solves the differential problem depends on the grid's step $h \sim \frac{1}{N}$, and the following asymptotic is fulfilled:

$$u_h(\vec{x}) = u(\vec{x}) + C(\vec{x})h^\nu + o(h^\nu) \quad (6)$$

Therefore, we obtain for the step $2h$:

$$u_{2h}(\vec{x}) = u(\vec{x}) + C(\vec{x})2^\nu h^\nu + o(h^\nu) \quad (7)$$

We obtain from estimations (6-7): $C(\vec{x}) = \dfrac{u_h(\vec{x}) - u_{2h}(\vec{x})}{(1-2^\nu)h^\nu}$, $u(\vec{x}) = u_{2h}(\vec{x}) - C(x)(2h)^\nu + o(h^\nu)$.

We compare two solutions $u_{2h}(\vec{x})$ и $u_h(\vec{x})$ only on the coarsest grid with step $2h$.

The compact scheme's accuracy order is equal to 4, therefore one should take $\nu = 4$.

Helmholtz equation

Compact approximation of Helmholtz Eq. (2) can be reduced to compact approximation of the Poisson equation by using the following substitution: $g = f - \rho(x, y)u$. We construct the global SLAE for u and g: $Au = Pg \Leftrightarrow (A + \bar{\rho}P)u = Pf \Leftrightarrow Bu = Pf$, where the matrix $B = A + P\bar{\rho}$, $\bar{\rho}$ - the diagonal matrix with grid values of the coefficient ρ in Eq. (2). If the function ρ is positive, then the spectrum of the Helmholtz operator will also be positive and matrix B will be well conditioned. Otherwise we can't guarantee good conditionality of matrix B.

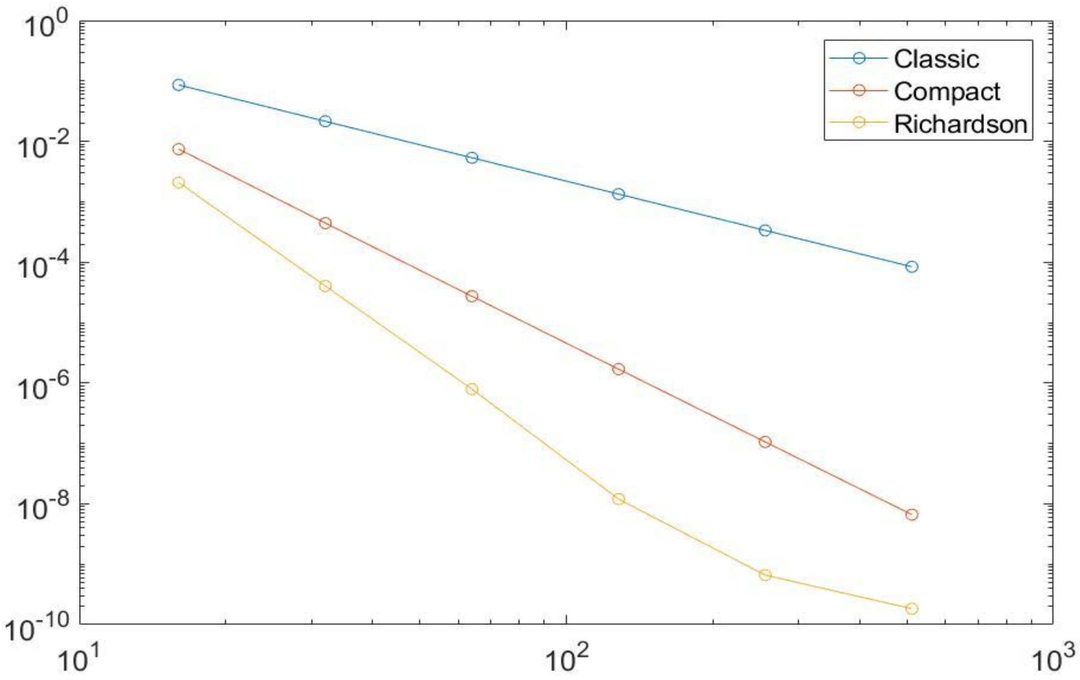

Fig.12. *The schemes' error depending on N in loglog coordinates for Helmholtz equation. Here* $\tilde{u} = x^6 \sin(y)$.
The coefficient

$$\rho(x, y) = \exp\left(-\frac{1}{y(y - 2\pi)}\right)$$

is positive.

Discontinuous coefficient ρ in Helmholtz equation.

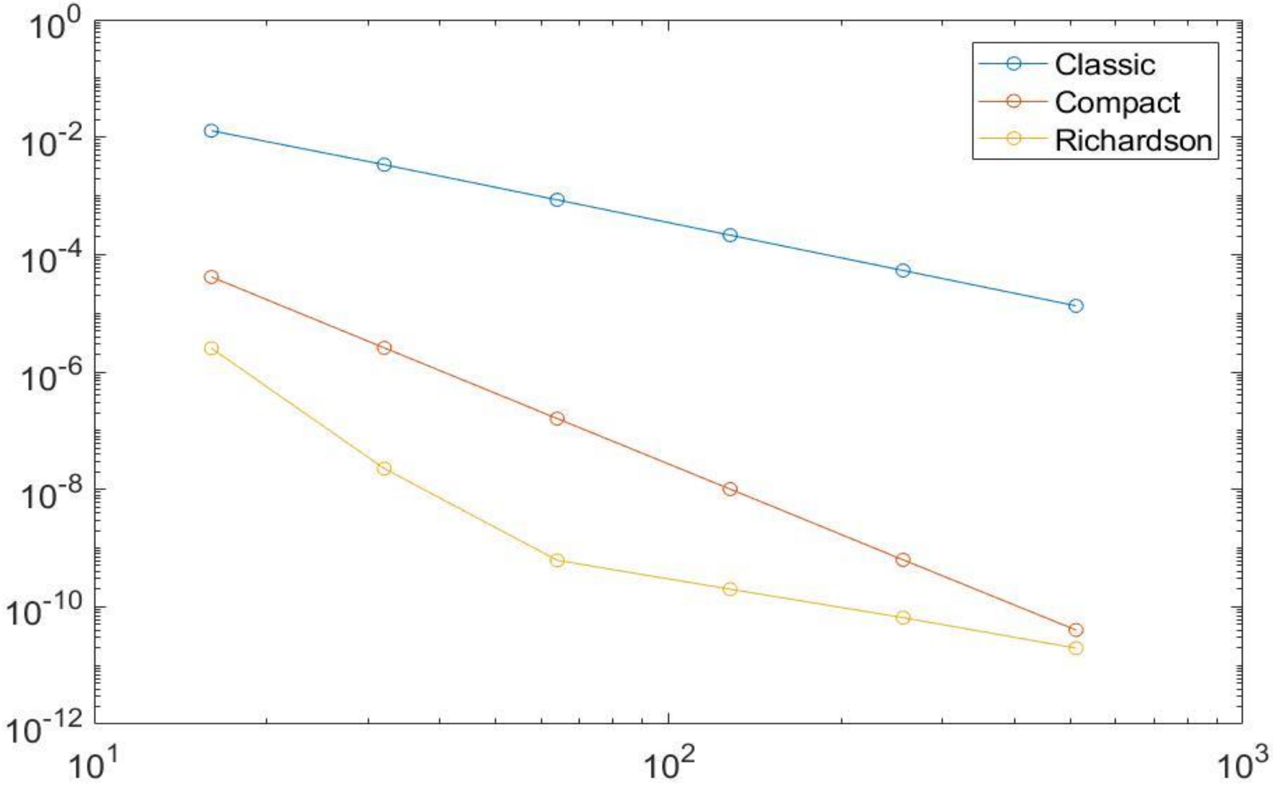

Fig.13. *The same results for*

$$\tilde{u} = \sin(y + x) + 2$$

and coefficient:

$$\rho(x, y) = \begin{cases} 1, & x \le 0 \\ 10, & x \ge 0 \end{cases}.$$

Complex coefficient ρ in the Helmholtz equation.

To provide well conditionality of matrix B one should take the function ρ with a positive real part.

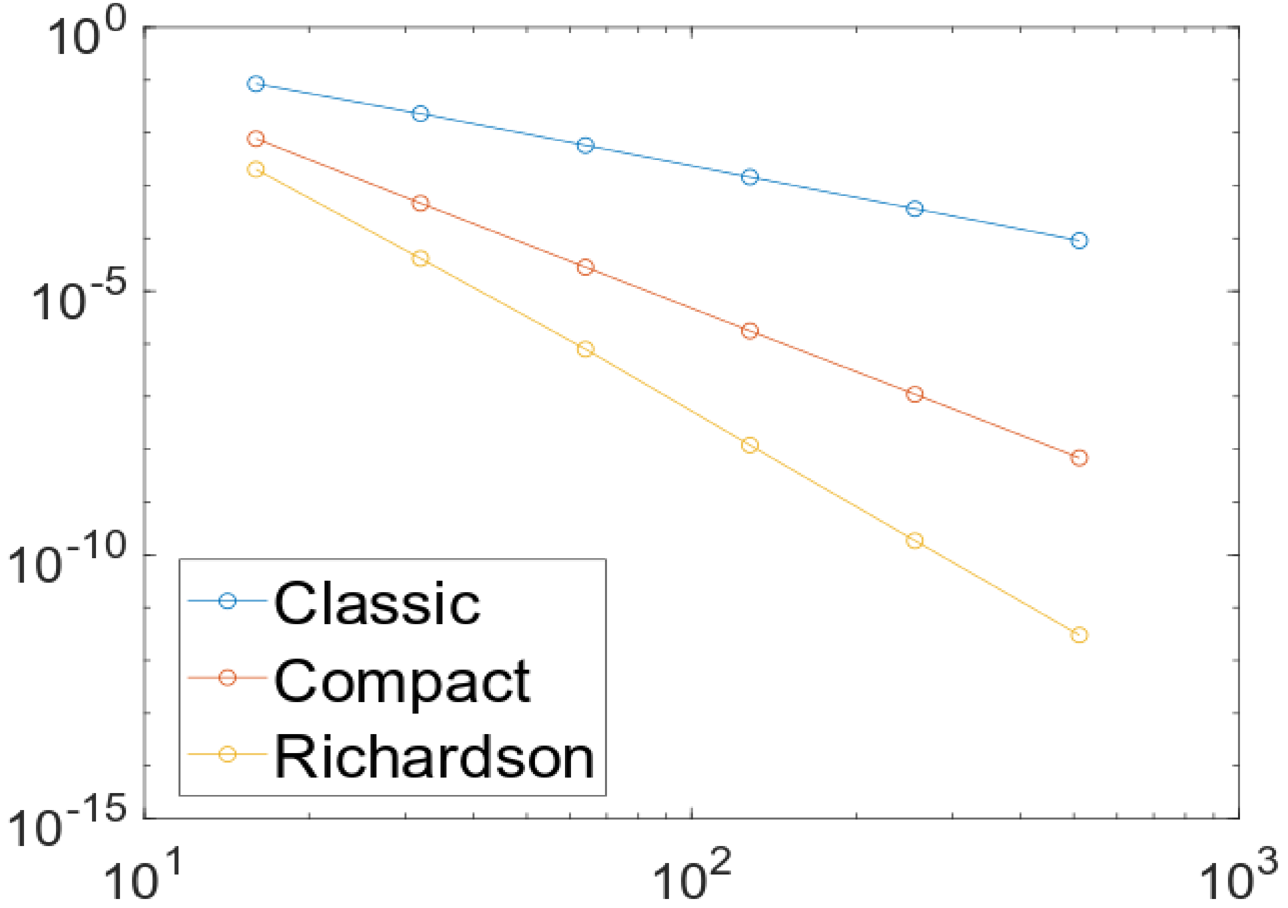

Fig.14. *The same results for* $\tilde{u} = \sin(y+x)+2$

and coefficient:

$$\rho = \exp(i(x+y))+2 .$$

Multigrid method

The idea of the multigrid method is that one needs to consistently apply several embedded into each other grids with resolutions N_0, $2N_0$, $4N_0$,...., $2^{k-1}N_0$, respectively. This method is effective as it allows to attenuate amplitudes of the problem's eigen functions rather fast for a wide diapason of wavenumbers. It happens so because each grid has its own diapason of fast attenuating eigen functions and the multigrid technic allows to combine them.

Transmission from a coarser grid to a finer: bilinear interpolation

Transmission from a finer grid to a coarser: simple restriction

We apply the grids in the following order:

Iterations start on the coarsest grid, which are followed by a series of refinements and smoothing relaxation iterations after each refinement. After that we start series of coarsening with smoothing iteration after each coarsening. This process is called a *V*-cycle. In this study we assume that the resolution of the coarsest grid $N_0 = 16$.

Мы экспериментально устанавливаем оптимальное (в смысле числа операций) соотношение между числом *V*-циклов *W* и шагом самой мелкой сетки N_{fin}.

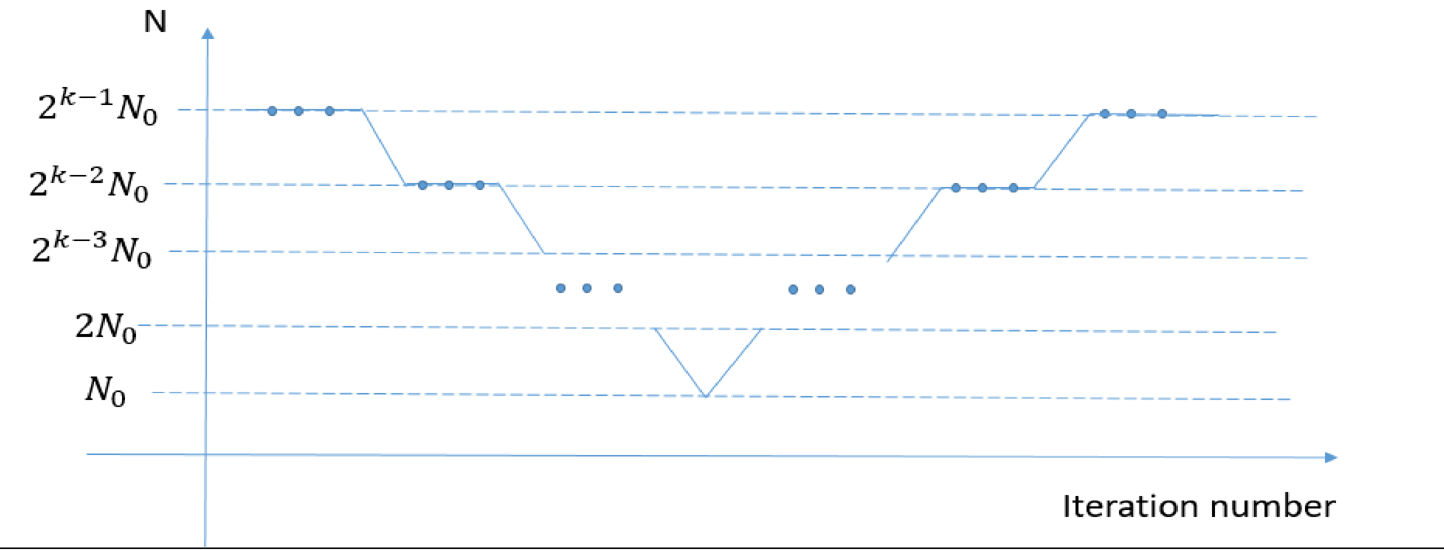

Fig.15. *Structure of a V-cycle.*

The efficiency of the multigrid method is described by two parameters: NN (normalized norm of the residual) and CC (computational cost – number of arithmetical operations +, -, /, *)

We provide below the results of experiments: NN and CC depending on the resolution of the finest grid.

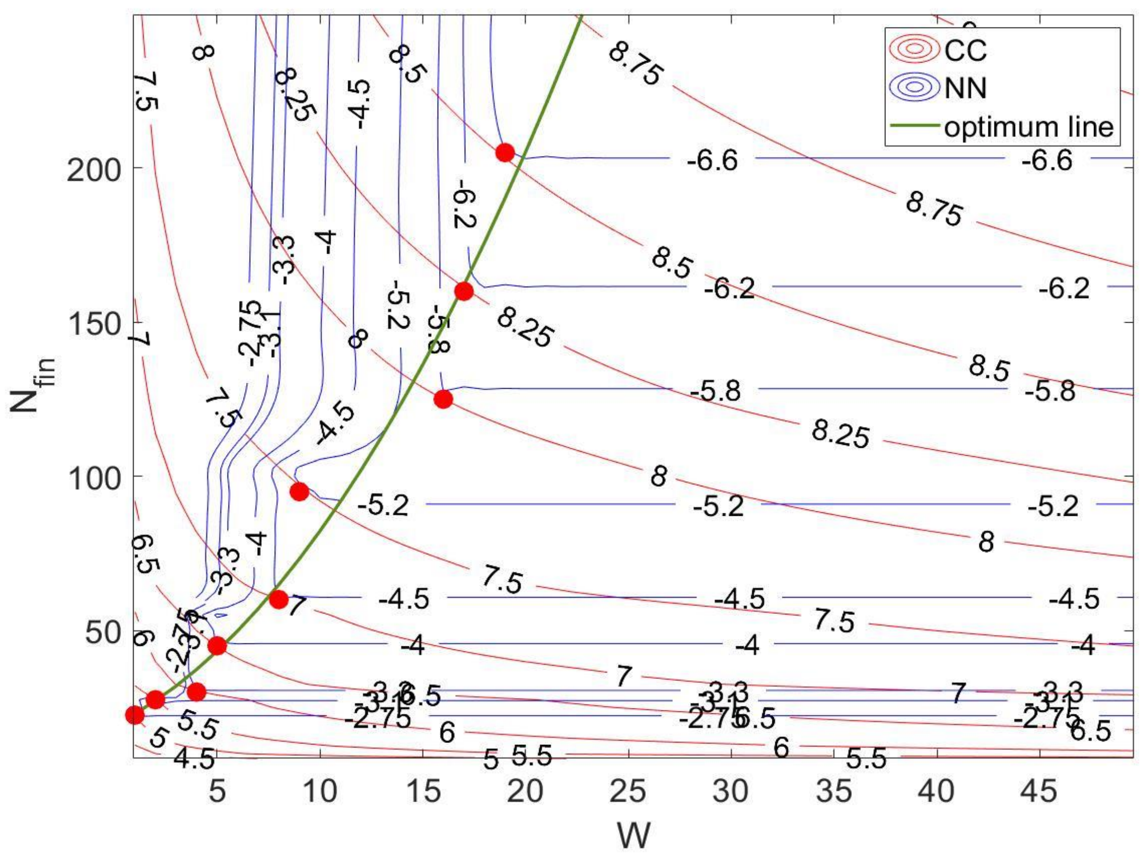

Fig.16. *Isolines of CC and NN for the compact scheme depending on the number of V-cycles (W) and the resolution of the finnest grid (* N_{fin} *). The green line shows the optimal realtinon between W and* N_{fin}.
Here $u = \sin(x + y)$

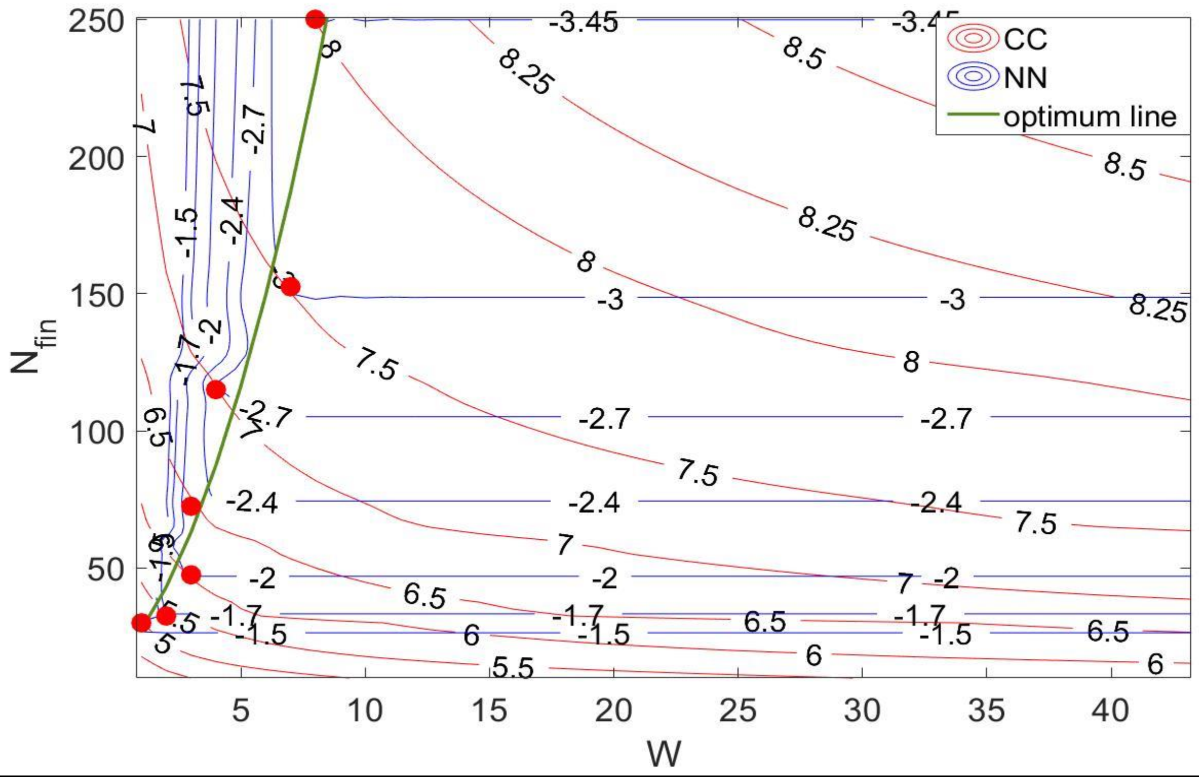

Fig.17. *Same results for the classic scheme.*

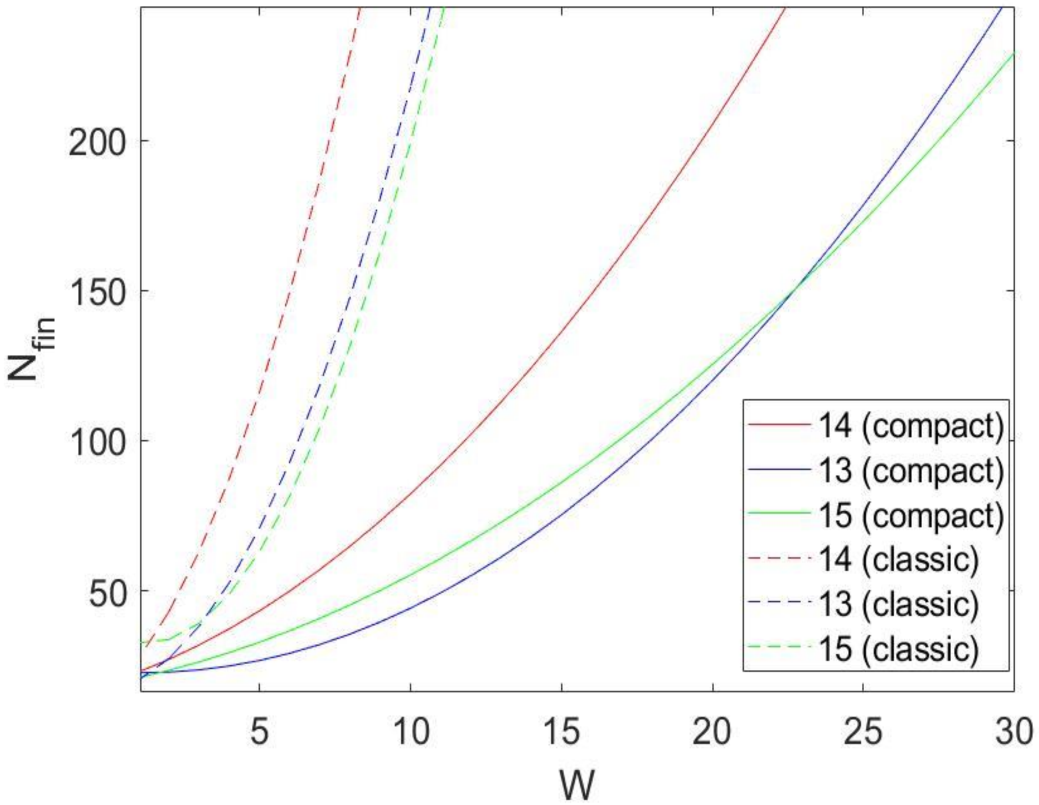

Fig.18. *Optimal curves for both schemes for various exact solutions:*

13) $\tilde{u} = \sin(x + y)$

14) $\tilde{u} = \sin(x)$

15) $\tilde{u} = x^6 \sin(y)$.

Acknowledgements

The study was prepared within the framework of the Academic Fund Program at the National Research University Higher School of Economics (HSE) in 2020 – 2021 (grant № 20-04-021) and by the Russian Academic Excellence Project 5-100.